

1 Constructing smaller genome graphs via string compression

2 Yutong Qiu¹ and Carl Kingsford^{1,2}

3 ¹ Carnegie Mellon University, Pittsburgh PA, 15213

4 ² carlk@cs.cmu.edu

5 **Abstract.** The size of a genome graph — the space required to store the nodes, their labels and
6 edges — affects the efficiency of operations performed on it. For example, the time complexity
7 to align a sequence to a graph without a graph index depends on the total number of characters
8 in the node labels and the number of edges in the graph. The size of the graph also affects
9 the size of the graph index that is used to speed up the alignment. This raises the need for
10 approaches to construct space-efficient genome graphs.

11 We point out similarities in the string encoding approaches of genome graphs and the external
12 pointer macro (EPM) compression model. Supported by these similarities, we present a pair
13 of linear-time algorithms that transform between genome graphs and EPM-compressed forms.
14 We show that the algorithms result in an upper bound on the size of the genome graph con-
15 structed based on an optimal EPM compression. In addition to the transformation, we show
16 that equivalent choices made by EPM compression algorithms may result in different sizes of
17 genome graphs. To further optimize the size of the genome graph, we propose the source as-
18 signment problem that optimizes over the equivalent choices during compression and introduce
19 an ILP formulation that solves that problem optimally. As a proof-of-concept, we introduce
20 RLZ-Graph, a genome graph constructed based on the relative Lempel-Ziv EPM compression
21 algorithm. We show that using RLZ-Graph, across all human chromosomes, we are able to
22 reduce the disk space to store a genome graph on average by 40.7% compared to colored de
23 Bruijn graphs constructed by Bifrost under the default settings.

24 The RLZ-Graph software is available at <https://github.com/Kingsford-Group/rlzgraph>

25 **Keywords:** Genome graph construction · String compression · Relative Lempel-Ziv.

26 1 Introduction

27 The linear reference genome suffers from reference bias that results in discarding informative reads
28 sequenced from non-reference alleles during alignment [Ballouz et al., 2019]. To reduce the reference
29 bias, alternative read alignment approaches that use a set of genomes as the reference have been
30 recently introduced [Chen et al., 2020, Novak et al., 2017]. Genome graphs, due to their compact
31 structure to store the shared regions of highly similar strings, are widely used to represent and ana-
32 lyze a collection of reference genomes compactly [Paten et al., 2017, Computational Pan-Genomics
33 Consortium, 2018, Sherman and Salzberg, 2020, Sherman et al., 2019].

34 A genome graph of a collection of sequences is a labeled directed graph such that each sequence
35 is equal to the concatenation of node labels on a path. We call such path a reconstruction path.
36 The size of a genome graph is the space to store the graph structure, which is the set of nodes,
37 edges and the node labels.

38 The size of a genome graph is crucial to the efficiency of operations such as mapping sequencing
39 reads. Shown in Jain et al. [2019], the time complexity of mapping a string to a genome graph is
40 directly correlated with the total number of characters in node labels and the number of edges. The
41 speed of sequence-to-graph mapping can be further improved by a graph index, the size of which
42 is also dependent on the size of the genome graphs. [Paten et al., 2017, Sirén et al., 2014, 2020].

43 Most of the existing genome graph construction algorithms do not directly optimize the size of
44 the genome graph. Some of these algorithms choose a type of graph in order to adapt to a specific
45 type of input data, such as read alignment [Garrison et al., 2018, Li et al., 2020, Paten et al., 2011,
46 Mäkinen et al., 2020], variant calls [Garrison et al., 2018, Rakocevic et al., 2019, Diltthey et al.,
47 2015] or raw sequencing reads [Iqbal et al., 2012], and then optimize the chosen graph. The other
48 only optimize the graph index that stores reconstruction paths based an assumed type of genome
49 graphs, for example, the variation graphs [Sirén et al., 2020, Sirén, 2017] or the colored compacted
50 de Bruijn graphs [Almodaresi et al., 2017, 2020, Holley and Melsted, 2020, Muggli et al., 2019,
51 Minkin et al., 2017]. As a result, the graphs constructed can be large in terms of both the space
52 taken by the graph structure or the lengths of the reconstruction paths.

53 While a small genome graph is desirable, the smallest genome graph may be useless if each edge
54 is allowed to be traversed multiple times. The smallest genome graph is a complete graph with
55 four nodes, or K_4 , whose labels are A , T , C and G , respectively, and contains the reconstruction
56 path for any genomic sequence. The strings stored in a genome graph are parsed into a sequence
57 of nodes on the reconstruction path. However, the parsing of strings would have lengths equal to
58 the lengths of the strings in K_4 , which undermines the goal of a genome graph to compactly store
59 similar strings.

60 In order to construct a small genome graph that balances the size of the graph and the lengths of
61 the reconstruction paths, we introduce the definition of a restricted genome graph and formalize the
62 restricted genome graph optimization problem, which seeks to build a smallest restricted genome
63 graph given a collection of strings.

64 We present a genome graph construction algorithm that directly addresses the restricted genome
65 graph size optimization problem. Optimizing the size of a restricted genome graph is similar to
66 optimizing the space taken by a set of strings, which echoes the external pointer macro (EPM)
67 scheme. We introduce a pair of algorithms that transform between the EPM-compressed form and
68 the restricted genome graphs, and prove an upper bound on the size of the restricted genome graph
69 constructed given an optimized EPM-compressed form from a set of input sequences. We further
70 reduce the number of nodes and edges in the constructed restricted genome graph by introducing
71 and solving the source assignment problem via integer linear programming (ILP).

72 As a proof-of-concept that compression-based genome graph construction algorithms produce
73 small genome graphs efficiently, we build the RLZ-Graph, which is based on an EPM scheme
74 compression heuristic known as the relative Lempel-Ziv (RLZ) algorithm. The EPM compression
75 problem is NP-complete [Storer and Szymanski, 1982]. Among the approximation heuristics to solve
76 the EPM compression problem, the relative Lempel-Ziv algorithm [Kuruppu et al., 2010] runs in
77 linear time and achieves good compression ratios on human genomic sequences [Deorowicz et al.,
78 2015, Deorowicz and Grabowski, 2011, Ferrada et al., 2014].

79 We evaluate the performance of RLZ-Graph by comparing to the colored compacted de Bruijn
80 graphs (ccDBG) [Iqbal et al., 2012]. CcdBG construction methods, similar to the compression-based
81 genome graph construction algorithms, process the input sequences directly without intermediate

82 steps such as alignment or variant calling. In ccdBG, the input sequences are fragmented into
83 preliminary nodes that represent unique strings of length k , or k -mers. Each edge represents the
84 adjacency between two k -mers in the sequences stored. The preliminary nodes with in- and out-
85 degrees equal to 1 on a path are further merged into a supernode. Still, the number of nodes and
86 edges, as well as the number of characters in node labels, in a ccdBG can increase significantly as the
87 number of sequences stored increases. The size of the graph also depends heavily on the parameter
88 k . These factors may offset the effort to efficiently encode the reconstruction path information in the
89 graph indices [Almodaresi et al., 2017, 2020, Holley and Melsted, 2020, Muggli et al., 2019, Minkin
90 et al., 2017]. Despite the different approaches to build the ccdBG indices, ccdBG construction
91 methods results in the same underlying de Bruijn graph structure. When we compare our algorithm
92 with ccdBG construction algorithms, we only compare the graph structure, which includes nodes,
93 edges and sequences stored in each node.

94 To examine the performance of RLZ-Graph, we compare sizes of the RLZ-Graph with the ccdBG
95 constructed by Bifrost [Holley and Melsted, 2020] on all human chromosome sequences from 100
96 individuals from the 1000 Genome Project [1000 Genomes Project Consortium, 2015]. The number
97 of nodes and edges produced by RLZ-Graph are reduced significantly compared with the ccdBG.
98 Across all chromosomes, the disk space taken to store the graph representation of 100 sequences is
99 on average reduced by 40.7% compared with the ccdBG built under the default settings.

100 Additionally, we evaluate the performance of the ILP solution to the source assignment prob-
101 lem on RLZ-Graphs constructed from *E. coli* genome sequences, for which many whole genome
102 sequences are available. We show that the solutions to the source assignment problem reduces the
103 number of nodes by around 8% on 300 *E. coli* genomes.

104 2 Definitions

105 2.1 Strings

106 Let s be a string. $s[b : e]$ denotes a substring starting from position b (inclusively) of s up to position
107 e (inclusively). We assume 0-indexing throughout this article. The length of s is denoted by $|s|$.
108 Concatenations of strings $\{s_1, \dots, s_n\}$ are denoted by $s' = s_1 \cdot s_2 \cdot \dots \cdot s_n$.

109 2.2 Genome Graphs

110 **Definition 1 (Genome graph).** A genome graph $G = (V, E, \ell)$ of a collection of strings $\mathcal{S} =$
 111 $\{s_1, s_2, \dots, s_n\}$ is a directed graph with node set V , edge set E , and node labels $\ell(u)$ for each node u .
 112 A genome graph of \mathcal{S} contains a collection of paths $\mathcal{P} = \{P_1, P_2, \dots, P_n\}$, where $p_i = v_1^i, v_2^i, \dots, v_{|P_i|}^i$
 113 , such that $s_i = \ell(v_1^i) \cdot \ell(v_2^i) \cdot \dots \cdot \ell(v_{|P_i|}^i)$ for all $s_i \in \mathcal{S}$. Such paths are called reconstruction paths.

114 The size of a genome graph $G = (V, E, \ell)$ is denoted by $size(G)$, which is the space to store
 115 the set of nodes, edges and node labels (Section 3.1). The number of nodes in node set V and the
 116 number of edges in edge set E are denoted as $|V|$ and $|E|$, respectively.

117 **Definition 2 (Restricted genome graph).** A restricted genome graph is a genome graph with
 118 a source and sink node and the restriction that each edge is allowed to be traversed at most once in
 119 all reconstruction paths.

120 An example of a restricted genome graph is shown in Figure 1. Each edge is traversed only
 121 once in all reconstruction paths, and parallel edges are present. In a restricted genome graph, if
 122 we insert the source and sink nodes to the beginning and the end of each reconstruction path and
 123 add edges directing from sink to source, then the concatenation of reconstruction paths for all
 124 sequences forms an Eulerian tour. For a restricted genome graph $G = (V, E, \ell)$ and a collection of
 125 all reconstruction paths $\mathcal{P} = \{P_1, P_2, \dots, P_n\}$, we have $|E| = \sum_{P_i \in \mathcal{P}} (|P_i| - 1) + 2n$, where $2n$ edges
 126 are the edges directing from source nodes and edges directing to sink nodes.

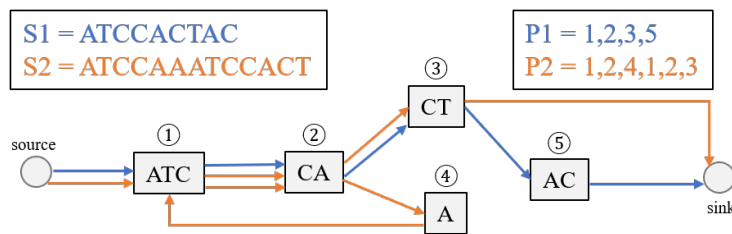


Fig. 1. An example of a restricted genome graph. The graph stores two strings, S1 and S2. The color of the edges denotes the origin of node adjacencies.

127 2.3 External Pointer Macro (EPM) Compression Scheme

128 We review the definition of the external pointer macro (EPM) scheme for data compression [Storer
 129 and Szymanski, 1982].

130 **Definition 3 (Pointers in EPM).** Given a reference string R , a pointer $p_i = (pos_i, len_i)$ repre-
131 sents the substring $R[pos_i : pos_i + len_i - 1]$.

132 We say that two pointers, $p_i = (pos_i, len_i)$ and $p_j = (pos_j, len_j)$ are equivalent to each other if
133 $R[pos_i : pos_i + len_i - 1] = R[pos_j : pos_j + len_j - 1]$.

134 **Definition 4 (External pointer macro (EPM) model).** Given an alphabet Σ and a string T ,
135 a compressed form of string T adopts the EPM if the compressed data follows the form $C = R\#t$,
136 where R is a string over Σ , $t = p_1p_2, \dots$ is a sequence of pointers that represent substrings in R , $\#$
137 is a separator symbol that is not in Σ , and T is equal to the string produced by substituting pointers
138 in t by their corresponding substrings.

139 The string T may represent a set of strings $S = \{s_1, s_2, \dots, s_n\}$ by concatenation, i.e. $T =$
140 $s_1\$s_2\dots\s_n , where $\$ \neq \#$ and $\$ \notin \Sigma$, where Σ is the alphabet for S . In this case, the compressed
141 form t will also contain the character $\$$ that separates sequences of pointers that represent different
142 strings.

143 It is natural to consider optimizing the size of the compressed string C , $size(C)$ (Section 3.2),
144 which leads to:

145 **Problem 1 (EPM decision problem [Storer and Szymanski, 1982]).** Given a string T
146 and an integer m , determine if there is a compressed form C of T that follows EPM such that
147 $size(C) \leq m$.

148 In Storer and Szymanski [1982], Problem 1 is shown to be NP-complete.

149 In EPM, the substring represented by a pointer may occur several times in the reference string.
150 We define such occurrences as sources of a pointer:

151 **Definition 5 (Source).** A source, (pos_1, len) , of a pointer $p = (pos_2, len)$ is an occurrence of
152 $R[pos_2 : pos_2 + len - 1]$ in R . In other words, $R[pos_1 : pos_1 + len - 1] = R[pos_2 : pos_2 + len - 1]$. Each
153 pointer p is associated with a source set $\mathcal{S}_p = \{ss_1, ss_2, \dots\}$, where $R[ss_i.pos : ss_i.pos + ss_i.len - 1] =$
154 $R[p.pos : p.pos + p.len - 1]$ for all $ss_i \in \mathcal{S}_p$.

155 Sources are used to refer to the occurrences of a substring on the reference string R , and pointers
156 are used to refer to the pair of integers eventually stored in the compressed string t .

157 **Definition 6 (Boundaries of sources and pointers).** *The boundaries of a source $s = (pos, len)$*
158 *are defined as (b, e) , where $b = pos$ and $e = pos + len$. b is the left boundary and e is the right*
159 *boundary. The similar definition of boundaries applies to pointers.*

160 Two boundaries, (b_1, e_1) and (b_2, e_2) , intersect if and only if $b_1 = b_2$ or $b_1 = e_2$ or $e_1 = b_2$ or
161 $e_1 = e_2$.

162 2.4 Relative Lempel-Ziv Algorithm

163 **Definition 7 (Right-maximal pointer).** *Given a reference string R and a string T , let pointer*
164 *$p = (pos, len)$ represent the substring $R[pos : pos + len - 1]$ and $T[pos' : pos' + len - 1]$. p is*
165 *right-maximal if $R[pos : pos + len] \neq T[pos' : pos' + len]$.*

166 **Definition 8 (Phrase).** *Given a reference string R and a string T , a phrase, $p = (pos, len)$, is a*
167 *right-maximal pointer.*

168 The relative Lempel-Ziv (RLZ) algorithm, proposed by [Kuruppu et al. \[2010\]](#), runs in linear
169 time and achieves good compression ratios with genomic sequences. RLZ takes a reference string R
170 as input and parses the input string T greedily from left to right. At position i in T , RLZ substitutes
171 the longest prefix of $T[i : |T| - 1]$ that matches a substring in R with a phrase. Let the length of the
172 phrase be len . After substitution, RLZ skips to position $i + len$ in T and repeats the substitution
173 process until T is exhausted. The process of phrase production is called RLZ factorization. In some
174 analysis of RLZ, the reference string is generated from the set of input strings [[Gagie et al., 2016](#)].
175 Nevertheless, the RLZ factorization algorithm given a reference string remains the same.

176 The definitions introduced above are demonstrated in Figure 2, where R is the reference string
177 and T is the input string to the RLZ algorithm. RLZ factors T into a sequence of three phrases,
178 shown as t . The compressed form of the input string T is $C = R\#t$. Each phrase is associated
179 with some sources that are represented as line segments in the figure. For example, the last phrase,
180 $(7, 2)$, replaces the substring $T[7 : 8]$. It also corresponds to two sources in R : $(3, 2)$ and $(7, 2)$, which
181 are represented by the green line segments in R . The left and right boundaries of phrase $(7, 2)$ are
182 $(b = 7, e = 8)$ in T . Source $(3, 2)$ intersects with sources $(1, 4)$ and $(3, 3)$. However, sources $(1, 4)$
183 and $(3, 3)$ do not intersect with each other.

	\emptyset	1	2	3	4	5	6	7	8
R =	A	T	C	G	A	T	A	G	A
sources									
T =	T	C	G	A	G	A	T	G	A
t =		(1,4)			(3,3)			(7,2)	

Fig. 2. An example of RLZ factorization. The top row is the indices of characters in the strings. R is the reference string, T is the input string and t is a sequence of phrases resulted from RLZ factorization. Colored line segments on the third row represent the sources associated with phrases with the same color.

184 3 Size formulation of restricted genome graphs and EPM-compressed forms

185 3.1 Size of a genome graph

186 We adopt a natural formulation of the size of a labeled graph, which describes the space to store
 187 nodes, edges and the node labels. Given a restricted genome graph $G = (V, E, \ell)$ over alphabet Σ ,
 188 let L be a string that contains every node label as a substring and Σ be the alphabet. Each node
 189 can be represented as a pointer to L , i.e. $v = (pos, len)$, such that $\ell(v) = L[pos : pos + len - 1]$.
 190 Each node takes $2 \log |L|$ bits to store. The graph structure is stored as pairs of adjacent nodes.
 191 Each edge takes space $2 \log |V|$ bits. Therefore, the total space taken by a restricted genome graph,
 192 denoted by $size(G)$, under this model is:

$$size(G) = |L| \cdot \log |\Sigma| + |V| \cdot 2 \log |L| + |E| \cdot 2 \log |V|. \quad (1)$$

193 We introduce the restricted genome graph optimization problem:

194 **Problem 2 (Restricted genome graph optimization problem).** Given a set of sequences,
 195 build a restricted genome graph G such that $size(G)$ is minimized.

196 In the above formulation, note that $|E|$ refers to the number of edges including the parallel
 197 edges. Solutions to Problem 2 avoid a trivial genome graph solution, that is a complete graph with
 198 four nodes, or K_4 , where each node has label A , T , C , and G , respectively. From K_4 , any sequence
 199 over the alphabet $\Sigma = \{A, T, C, G\}$ can be reconstructed under the definition of a genome graph
 200 (Definition 1). However, the length of the reconstruction path would be equal to the length of the
 201 sequence, which undermines the purpose of the genome graph, part of which is to produce a short
 202 parsing of the input sequence.

203 In a restricted genome graph, the number of edges grows as the lengths of reconstruction
204 paths increase. Therefore, minimizing the size of the restricted genome graph achieves a combined
205 objective of a small genome graph and short parsing of the input sequences.

206 3.2 Size of an EPM-compressed form

207 Next, we consider the space taken by an EPM-compressed form $C = R\#t$. The space taken by
208 C , $size(C)$, is the space to store the total number of unique pointers in t , the sequence t and the
209 reference string R . We first encode each unique pointer with a pair of integers, (pos, len) , which
210 takes space $2 \log |R|$ bits. If there are n unique pointers, t can be stored as a sequence of identifiers
211 of the unique pointers using $|t| \log n$ bits. Therefore, the total space taken by an EPM-compressed
212 form is

$$size(C) = |R| \cdot \log |\Sigma| + |t| \cdot \log n + n \cdot 2 \log |R|. \quad (2)$$

213 From equations (1) and (2), both the restricted genome graph and the EPM-compressed form
214 have a size formulation that has three terms, which are the space taken by a reference string, the
215 space taken by the unique pointers and the space to store the adjacencies between pointers.

216 In order to reduce the size of the restricted genome graphs (Definition 2), it is natural to
217 borrow ideas from the field of string compression. We introduce two algorithms that transform
218 between genome graphs and compressed strings produced by EPM compression scheme [Storer and
219 Szymanski, 1982].

220 4 Transformation between EPM-compressed forms and genome graphs

221 4.1 EPM-compressed string to genome graph

222 Given an EPM-compressed form $C = R\#t$ of the original string T , and an alphabet Σ , the genome
223 graph construction algorithm produces a restricted genome graph that stores both R and T .

224 A naïve algorithm to construct a genome graph is to create a node for each unique pointer in
225 t and add an edge between nodes that represent each pair of pointers $t[i]$ and $t[i + 1]$. However,
226 in repetitive sequences such as the human genome, a substring may occur in several pointers and
227 thus may be stored several times redundantly. In the example shown in Figure 3, the substring AAA

$$R = AAATCG$$
$$S = \underline{AAA} \underline{AAAT} \underline{AAATC}$$

Fig. 3. String S is factored into three pointers given the reference string R . Each underlined substring is represented by a different pointer. According to the naïve algorithm to construct the genome graph, three nodes are created from three pointers.

228 would be stored three times according to the naïve algorithm, which results in excess space spent
229 on storing repetitive content.

230 Our construction algorithm, introduced below as **two-pass CtoG**, merges the repetitive sub-
231 strings shared by multiple pointers by grouping pointers by their positions on the reference. “Two-
232 pass CtoG” creates nodes and edges of the genome graph in two passes through t . In the first pass,
233 the algorithm creates nodes by cutting the reference string according to the boundaries of each
234 pointer. In the second pass, the algorithm connects the nodes according to the adjacencies between
235 pointers in the compressed string t .

236 **First pass.** Create a bit vector, \mathcal{B} . A bit set at $\mathcal{B}[i]$ indicates that a pointer boundary falls at
237 position i on R . Process t from left to right. For each pointer $p = (pos, len)$, mark its boundaries in
238 \mathcal{B} : $\mathcal{B}[pos] = 1$ and $\mathcal{B}[pos + len] = 1$. After t is exhausted, transform \mathcal{B} into an RRR data structure
239 that supports **rank** operations in constant time [Raman et al., 2002], where $\text{rank}_{\mathcal{B}}(i)$ returns the
240 number of set bits at or before position i in \mathcal{B} . We then cut reference string at positions where
241 a bit is set in \mathcal{B} . If $\mathcal{B}[i]$ and $\mathcal{B}[j]$ are the only set bits in the interval $[i : j]$, we create a node
242 $v = (pos, len) = (i, j - i)$ with $\ell(v) = R[i : j - 1]$. Each node can be treated as a pointer whose left
243 and right boundaries are i and j , respectively. Each node is identified using its left boundary, i.e.
244 $\text{rank}_{\mathcal{B}}(i)$.

245 We define the ordering of nodes. $v_i = (pos_i, len_i) \prec v_j = (pos_j, len_j)$ iff $pos_i < pos_j$, where
246 i and j are the identifiers of v_i and v_j , and $i < j$. Add an edge between each v_i and v_{i+1} for all
247 $i < |V| - 1$. The path $v_1, v_2, \dots, v_{|V|}$ represents the reference string R .

248 **Second pass.** We process t from left to right again in the second pass. For each pair of pointers
249 $t[i]$ and $t[i + 1]$, we need to connect the nodes that mark the right and left boundaries of $t[i]$ and
250 $t[j]$, respectively. Let $t[i] = (pos_i, len_i)$ and $t[i + 1] = (pos_{i+1}, len_{i+1})$. We need to find two nodes,
251 $v_m = (pos_m, len_m)$ and $v_n = (pos_n, len_n)$, such that $pos_m + len_m = pos_i + len_i$ and $pos_n = pos_{i+1}$.

252 Since each node is identified by their left boundary, two nodes can be identified by $m = \mathbf{rank}_{\mathcal{B}}(\mathit{pos}_i +$
253 $\mathit{len}_i - 1)$ and $n = \mathbf{rank}_{\mathcal{B}}(\mathit{pos}_{i+1})$. Edge (v_m, v_n) then represents the adjacency between $t[i]$ and $t[i+1]$
254 in t . Repeat the process until t is exhausted. Create a source and a sink node. Create an edge that
255 connects the source to the first node of each compressed string and the last node of each compressed
256 string to the sink. An example output of the algorithm is shown in Figure 4, where the compressed
257 string is produced by the RLZ algorithm [Kuruppu et al., 2010].

258 The running time of the construction algorithm is $O(|t| + |R|)$, where $|t|$ is the total number
259 of pointers. In both passes, the algorithm iterates through all pointers in t exactly once. Since
260 the nodes are created by splitting the reference, there are at most $|R|$ nodes and adding an edge
261 between each pair of (v_i, v_{i+1}) takes $O(|R|)$ time.

262 The constructed restricted genome graph stores the set of nodes, edges and the node labels.
263 While storing the reconstruction paths is also important, it is a separate challenge from optimizing
264 the graph structure. There has been a line of work that constructs small graph indices to store
265 the reconstruction paths efficiently given any graph structure [Sirén et al., 2014, 2020, Sirén, 2017].
266 These indices can also be applied to our genome graph.

267 There are three types of edges in the produced restricted genome graph: the backward edges,
268 the forward edges and the reference edges. We define the backward edges as edges that direct from
269 v_j to v_i , where $j \geq i$, which include self-loops. We define the forward edges as edges that direct
270 from v_i to v_j , where $i < j - 1$. We define the reference edges as the edges that direct from v_i to
271 v_{i+1} . In other words, reference edges $(v_i = (\mathit{pos}_i, \mathit{len}_i), v_j = (\mathit{pos}_j, \mathit{len}_j))$ connect nodes where the
272 first node's right boundary intersects with the second node's left boundary, i.e. $\mathit{pos}_i + \mathit{len}_i = \mathit{pos}_j$.

273 We show that the constructed graph is a restricted genome graph that contains reconstruction
274 paths for R and T as in Theorem 1.

275 **Theorem 1.** *Given an EPM-compressed form of string T , $C = R\#t$, the algorithm described above*
276 *creates a genome graph $G = (V, E, \ell)$ that contains reconstruction paths for R and T .*

277 *Proof.* In the second pass of the algorithm, edges are added between the nodes that are the suffix
278 and the prefix of adjacent pointers. Therefore, all pointer adjacencies are represented as edges in
279 the genome graph.

280 All substrings $R[i : j]$ can be reconstructed from G . If $R[i : j]$ is a substring of a node label,
281 it can be reconstructed from G . If $R[i : j]$ spans two nodes, it spans two nodes connected by a
282 reference edge.

283 Any substring $T[i : j]$ can be reconstructed from G . Suppose position i lands in the middle of
284 a pointer $p_k = (pos_k, len_k)$, which means that $k \leq i \leq k + len_k - 1$.

285 1. If $j \leq k + len_k - 1$, which means that $T[i : j]$ is a substring of the string represented by a
286 pointer. Since all pointers in t point to substrings in R and R can be reconstructed from G , a
287 substring of a pointer can be reconstructed.

288 2. If $j > k + len_k - 1$, which means that $T[i : j]$ spans at least two pointers. From the previous
289 case, we have that $T[i : k + len_k - 1]$ can be reconstructed using nodes and edges in G . Since
290 all adjacencies between two pointers are represented in G , we can apply the analysis to the rest
291 of $T[i : j]$. Therefore $T[i : j]$ can be reconstructed if it spans more than one pointer.

292 □

293 4.2 Genome graph to EPM-compressed form

294 Given a restricted genome graph $G = (V, E, \ell)$ and a set of reconstruction paths \mathcal{P} that represent
295 strings in \mathcal{S} , we present an algorithm, **GtoC**, that produces an EPM-compressed form $C = R\#t$
296 whose decompression equals string T , which is a concatenation of strings in \mathcal{S} .

297 Produce the reference string R by concatenating the node labels in an arbitrary order \mathcal{O} .
298 Each node can then be represented as a pointer to R and be denoted as $v_i = (pos_i, len_i)$, where
299 $\ell(v_i) = R[pos_i : pos_i + len_i - 1]$. Assign an identifier to each node such that for v_i and v_j , $i < j$ if
300 $pos_i < pos_j$.

301 Process all $P \in \mathcal{P}$ by substituting nodes with their pointer representations. If two adjacent
302 nodes v_i and v_j in P are connected by a reference edge, merge the two nodes into one pointer
303 $p = (pos_i, len_i + len_j)$. Concatenate all processed P , which results in t . The converted sequence of
304 pointers t is then $p_1, p_2, \dots, p_{|t|}$, where $|t| \leq \sum_{P \in \mathcal{P}} |P|$.

305 The converted C satisfies the EPM definition where R is a string over Σ and t is a sequence of
306 pointers to substrings in R . Since the concatenation of paths in \mathcal{P} spells out T by concatenating

307 all the labels of nodes on the path, substituting the pointers in t with corresponding substrings
308 reconstructs T .

309 The running time of the construction algorithm is $O(|V| + \sum_{P \in \mathcal{P}} |P|) = O(|V| + |E|)$.

310 The size of the produced EPM-compressed form can be further reduced if the reference string R
311 is equal to the shortest superstring that contains all the node labels. However, finding the shortest
312 superstring is a NP-hard problem when the number of nodes is greater than 2 and would be
313 impractical in dealing with large genomes.

314 5 Upper-bound on the size of the restricted genome graph and the 315 EPM-compressed form

316 We show that the size of a restricted genome graph G produced using the `two-pass CtoG` algorithm
317 is bounded by the terms of the input EPM-compressed form C (Lemma 1).

318 **Lemma 1.** *Given an optimally compressed EPM form $C = R\#t$, the size of the transformed*
319 *restricted genome graph $G = (V, E, \ell)$, $size(G)$, according to `two-pass CtoG` in Section 4.1 has an*
320 *upper bound:*

$$\begin{aligned} size(G) \leq & |R| \cdot \log |\Sigma| + \min(2n, |R|) \cdot 2 \log |R| \\ & + (\min(2n, |R|) \cdot |t| - 1) \cdot 2 \log(\min(2n, |R|)) \end{aligned} \quad (3)$$

321 where n is the number of unique pointers in t .

322 *Proof.* The algorithm introduced in Section 4.1 creates nodes by cutting the reference string R
323 according to boundaries of pointers. Each node is stored as a pointer (pos, len) to R , which takes
324 $2 \log |R|$ bits.

325 The total number of nodes produced by cutting the reference is $\leq \min(2n, |R|)$. The number of
326 cuts introduced by each unique pointer is ≤ 2 . The maximum number of nodes given a reference
327 string R is $|R|$. Therefore, the space to store all the nodes is $\leq \min(2n, |R|) \cdot 2 \log |R|$.

328 The total number of edges, including reference and non-reference edges, in a restricted genome
329 graph is $\leq \min(2n, |R|) \cdot |t| - 1$. After the first pass of `two-pass CtoG`, the interval corresponding
330 to each pointer may be cut into several nodes. Let the average number of nodes contained in each

331 pointer's interval be $a \leq |V| \leq \min(2n, |R|)$. The average number of reference edges within each
332 pointer is then $a - 1$. The total number of edges between pointers is $|t| - 1$, and the total number
333 of edges within pointers is $(a - 1) \cdot |t|$. Together, the number of edges in the reconstruction path is
334 $a \cdot |t| - 1 \leq \min(2n, |R|) \cdot |t| - 1$.

335 The size of the genome graph is then:

$$\begin{aligned} \text{size}(G) &= |R| \cdot \log |\Sigma| + |V| \cdot 2 \log |R| + |E| \cdot 2 \log |V| \\ &\leq |R| \cdot \log |\Sigma| + \min(2n, |R|) \cdot 2 \log |R| + (\min(2n, |R|) \cdot |t| - 1) \cdot 2 \log(\min(2n, |R|)). \end{aligned}$$

336 □

337 In practice, the graphs are stored such that the parallel edges are merged. We show that the
338 size of the genome graph G' produced by merging the parallel edges in G can also be bounded by
339 the terms of the EPM-compressed form C (Lemma 2).

340 **Lemma 2.** *Given a restricted genome graph, $G = (V, E, \ell)$, constructed from an optimally com-*
341 *pressed EPM form $C = R\#t$, the size of the genome graph, $G' = (V, E', \ell)$, produced by merging*
342 *parallel edges in G has an upper bound:*

$$\text{size}(G') \leq |R| \cdot \log |\Sigma| + \min(2n, |R|) \cdot 2 \log |R| + (\min(2n, |R|) + |t|) \cdot 2 \log(\min(2n, |R|)), \quad (4)$$

343 where n is the number of unique pointers in t .

344 *Proof.* Merging parallel edges does not change the number of nodes and the concatenation of node
345 labels.

346 The number of reference edges in G' is equal to $|V| - 1$, as the nodes are produced by cutting
347 the reference string.

348 The number of forward and backward edges in G is equal to $|t| - 1$, and the number of forward
349 and backward edges in G' is $\leq |t| - 1$ due to parallel edge merging. According to `two-pass CtoG`,
350 since C is optimal, only a forward or a backward edge can be added for each pair of adjacent pointers
351 in t during the second pass. Suppose two adjacent pointers, $p_1 = (\text{pos}_1, \text{len}_1)$ and $p_2 = (\text{pos}_2, \text{len}_2)$,
352 result in a reference edge, which means that $\text{pos}_2 = \text{pos}_1 + \text{len}_1$, the two pointers can be merged

353 into $p_3 = (pos_1, len_1 + len_2)$. Merging two pointers reduces the size of C , which contradicts the
 354 assumption that the size of C is optimal.

355 Together, the space to store all the edges in G' is $\leq |V| + |t| \leq (\min(2n, |R|) + |t|) \cdot 2 \log \min(2n, |R|)$.

356 Therefore, the size of the genome graph G' after merging the parallel edges in G is:

$$\begin{aligned} |G'| &= |R| \cdot \log |\Sigma| + |V| \cdot 2 \log |R| + |E'| \cdot 2 \log |V| \\ &\leq |R| \cdot \log |\Sigma| + \min(2n, |R|) \cdot 2 \log |R| + (\min(2n, |R|) + |t|) \cdot 2 \log (\min(2n, |R|)). \end{aligned}$$

357 □

358 We show in Lemma 3 that the size of the EPM-compressed form produced by GtoC algorithm
 359 (Section 4.2) is upper-bounded by the terms of the size of a restricted genome graph.

360 **Lemma 3.** *Given a restricted genome graph $G = (V, E, \ell)$ of a collection of strings \mathcal{S} , the size of*
 361 *the transformed EPM-compressed form of the concatenated strings in \mathcal{S} , $C = R\#t$ according to*
 362 *GtoC described in Section 4.2 has an upper bound:*

$$size(C) \leq |R| \cdot \log |\Sigma| + |E| \cdot \log \binom{|V| + 1}{2} + 2 \binom{|V| + 1}{2} \log |R|, \quad (5)$$

363 where R is a string formed by concatenating all node labels.

364 *Proof.* Let the set of paths corresponding to the set of strings \mathcal{S} be $\mathcal{P} = \{P_1, P_2, \dots, P_m\}$, where m
 365 is the number of strings in \mathcal{S} . Since G has an optimal size, the number of edges in G is exactly
 366 $|E| = \sum_{i \in [1, m]} (|P_i| - 1) + 2m = \sum_{i \in [1, m]} |P_i| + m$, where E includes reference, forward and backward
 367 edges. Note that if an edge does not belong to any path in \mathcal{P} , it can be eliminated in the graph,
 368 which results in a smaller restricted genome graph.

369 According to GtoC, the pointers are created by either directly converting a node or merging two
 370 nodes connected by a reference edge in a path $P \in \mathcal{P}$. Let the number of reference edges be r . The
 371 number of pointers in t , or $|t|$, is equal to $\sum_{i \in [1, m]} |P_i| - r = |E| - m - r < |E|$.

372 Given $|V|$ nodes, the reference constructed by concatenating all node labels contains $|V| + 1$
 373 cut positions including the positions before $R[0]$ and after $R[|R| - 1]$. From these cut positions, we

374 can produce at most $\binom{|V|+1}{2}$ pointers by selecting two positions as boundaries of a pointer. Let the
375 total number of unique pointers be n . Then $n \leq \binom{|V|+1}{2}$.

376 Together, the size of the EPM-compressed form is:

$$\text{size}(C) = |R| \cdot \log |\Sigma| + |t| \cdot \log n + n \cdot 2 \log |R| \quad (6)$$

$$\leq |R| \cdot \log |\Sigma| + |E| \cdot \log \binom{|V|+1}{2} + \binom{|V|+1}{2} \cdot 2 \log |R|. \quad (7)$$

377 □

378 The pair of algorithms do not produce an optimal genome graph or optimal EPM-compressed
379 form. Still, given an optimal input, the pair of algorithms achieve results that are bounded by the
380 original terms in the input. We further improve the transformation from EPM-compressed form to
381 genome graph by addressing the source assignment problem introduced below.

382 6 Source assignment problem

383 In an EPM-compressed form $C = R\#t$, each pointer may be associated with a substring that
384 occurs several times in R . We name such occurrences as sources. A source (pos_i, len_i) is assigned
385 to a pointer p if $p = (pos_i, len_i)$.

386 In the EPM formulation, assigning different sources to a pointer does not change the size of the
387 compressed string. However, the assignment of sources may affect the number of nodes significantly.
388 According to the **two-pass CtoG** algorithm, the number of cuts made in the reference is equal to
389 the number of distinct pointer boundaries. Therefore, the choice of sources is directly related to
390 the number of nodes in the graph. An example is illustrated in Figures 2 and 4. The last phrase,
391 $(7, 2)$, is associated with two sources, $(3, 2)$ and $(7, 2)$. If we assign $(3, 2)$ to the phrase, which is
392 different from the case in Figure 2, the number of nodes created will be 5. Otherwise, 6 nodes will
393 be created as in Figure 4.

394 Given an EPM-compressed form and the set of sources corresponding to each pointer, if we
395 can assign sources such that the total number of unique pointer boundaries is minimized, we can
396 reduce the size of the created graph. We formulate the source assignment problem and present

397 an integer linear programming (ILP) solution for the optimal source assignment in genome graph
398 construction.

399 **Problem 3 (Source assignment problem).** Given a collection of sources sets $\mathcal{S} = \{S_1, S_2, \dots, S_n\}$,
400 where S_i denotes the set of sources for a unique pointer i , find a set of sources S' such that for all
401 S_i , $S_i \cap S' \neq \emptyset$ and $|\bigcup_{s_m \in S'} \{b_m, e_m\}|$ is minimized, where b_m, e_m are boundaries of source m .

402 In this problem, we choose one source for each pointer such that the union of boundaries
403 $\{b_m, e_m\}$ of each chosen source $s_m = (pos_m, len_m)$ is minimized. As a reminder, $b_m = pos_m$ and
404 $e_m = pos_m + len_m$.

405 For convenience, we denote the union of boundaries in a source set S by $\bigcup_B \{S\}$, which is
406 equivalent to $\bigcup_{s_m \in S} \{b_m, e_m\}$.

407 The formulation of the source assignment problem is similar to the hitting set problem in that it
408 chooses the minimum number of positions to hit every pointer. However, the objective is indirectly
409 related to the number of the chosen sources, and the sources and pointers are defined in a string
410 context. The hardness of the source assignment problem is open due to these differences from the
411 setting of the hitting set problem. Still, the similarities to the hitting set problem lead to the
412 formulation of an integer linear programming solution.

413 6.1 Integer linear programming formulation

414 The objective of the ILP is to minimize the number of cuts made in the reference, where each cut
415 is made at the boundaries of chosen sources. For each chosen source $s = (pos_i, len_i)$, a cut is placed
416 at positions pos_i and $pos_i + len_i$, which are left and right boundaries of s .

417 We first construct a set of integers I that is the union of all source boundaries. Create a binary
418 variable x_p for each $p \in I$. x_p is set to one if a cut is made at position p .

419 We create a binary variable y_{s_i} for each source $s_i = (pos_i, len_i)$ that indicates whether the
420 source is chosen. We create a constraint (Inequality 9) that at least one source is chosen from each
421 set. We create another set of constraints (Inequalities 10,11) that ensures that if a source is chosen,

422 two cuts are made at its left (pos_i) and right ($pos_i + len_i$) boundaries. This leads to the ILP:

$$\min \sum_{p \in I} x_p \quad (8)$$

subjects to

$$\sum_{s_j \in S_i} y_{s_j} \geq 1 \quad \forall S_i \in \mathcal{S} \quad (9)$$

$$y_{s_j} \leq x_{pos_j} \quad (10)$$

$$y_{s_j} \leq x_{pos_j + len_j} \quad (11)$$

$$x_p, y_{s_j} \in \{0, 1\} \quad (12)$$

423 6.2 Pruning to reduce the number of sources

424 In practice, a pointer with a short length may correspond to a large number of sources. For example,
 425 a pointer with length one may correspond to $|R|/4$ sources, where R is the reference string when
 426 the alphabet size is 4. This could result in a huge number of variables in the ILP formulation and
 427 would hinder its practicality significantly.

428 To address this, we preprocess the sources as follows. If a source does not intersect with any
 429 other sources of different pointers, we eliminate the source from the source set unless it is the only
 430 source of a pointer. We name the eliminated sources isolated sources. Removing such sources does
 431 not affect the optimality of the solution.

432 **Lemma 4.** *If a set of sources, S , that satisfies the constraints of the source assignment problem,*
 433 *includes an isolated source s , it is possible to find a set of sources S' with equal or lower objective*
 434 *value that does not include s .*

435 *Proof.* Let the pointer for the isolated source be p and the source set of p be S_p . Since s is an
 436 isolated source, there must be at least another source s' in S_p . If s' also does not intersect with
 437 any other sources in S , $S' = |\bigcup_B \{(S \setminus s) \cup s'\}| = |\bigcup_B \{S\}|$. Otherwise, if s' intersects with some
 438 sources in S , this means that the union of source boundaries is reduced by at least 1 if we replace
 439 s with s' , i.e. $S' = |\bigcup_B \{(S \setminus s') \cup s\}| \leq |\bigcup_B \{S\}| - 1$. Therefore, excluding all isolating sources
 440 during preprocessing does not affect the optimality of the solution. \square

441 7 Relative Lempel-Ziv Graph

442 As a proof-of-concept that constructing a genome graph using a compression scheme results in small
443 graphs, we implement the graph construction algorithm based on an EPM compression scheme
444 algorithm, relative Lempel-Ziv. Given a reference string R , the relative Lempel-Ziv (RLZ) algo-
445 rithm [Kuruppu et al., 2010], introduced in Section 2.4, seeks to greedily produce a compressed
446 form of R where all pointers in R are right-maximal. We name the right-maximal pointers phrases.
447 RLZ factorization in this manuscript is done on the compressed suffix array in the SDSL C++
448 library [Gog et al., 2014].

449 We apply the two-pass CtoG algorithm described in Section 4.1 to construct a RLZ-Graph.
450 We merge the parallel edges in the implementation as it is the common practice in genome graph
451 storage.

452 An example of RLZ-Graph is shown in Figure 4. The RLZ-Graph is constructed based on the
453 RLZ factorization in Figure 2, where the reference string is $R = ATCGATAGA$, the input string
454 is $T = TCGAGATGA$ and the factored phrase sequence is $t = (1, 4), (3, 3), (7, 2)$. The nodes are
455 produced by segmenting R according to the boundaries of sources assigned to phrases in t .

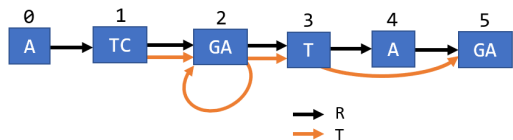


Fig. 4. The RLZ-Graph of reference $R = ATCGATAGA$ and input string $T = TCGAGATGA$ (Figure 2). The black path 0, 1, 2, 3, 4, 5 encodes R , the orange path 1, 2, 2, 3, 5 encodes T . The parallel edges are shown for the purpose of illustration and are merged in the final graph.

456 In the implementation of RLZ-Graph, we build a bi-directed graph where each node can be
457 traversed in forward and reverse directions, which is a commonly applied technique in other genome
458 graph construction algorithms. For each node $v = (pos, len)$, pos is referred to as the head of the
459 node and $pos + len$ is referred to as the tail. If a node is traversed in reverse direction, its label is
460 denoted as $\hat{\ell}(v)$, which is equal to the reverse complement of $\ell(v)$. This technique is useful in genomic
461 sequences that underwent structural variations such as inversions, where the entire genomic segment
462 is replaced by its reverse complement due to a double-strand break. During the construction of the
463 RLZ-Graph, we use a modified reference sequence R by concatenating the reference genome of the

464 organism of interest with its reverse complement. Before the source assignment step, we mark each
465 source as reversed if it is located on the reverse complement half of R and translate its boundary
466 positions to the forward half. After the source assignment step, we mark a pointer as reversed if it
467 is assigned a reversed source. When we add edges, if we encounter a reverse pointer $p = (pos, len)$,
468 we add an edge directing to the tail of the node $v_i = (pos_i, len_i)$ and an edge directing from the
469 head of the node $v_j = (pos_j, len_j)$, where $pos_i = pos$ and $pos_j + len_j = pos + len$.

470 We ran all our experiments on a server with 24 cores (48 threads) of two Intel Xeon E5 2690
471 v3 @ 2.60GHz and 377 GB of memory. The system was running Ubuntu 18.04 with Linux kernel
472 4.15.0.

473 **7.1 Performance of RLZ-Graph compared to the colored compacted de Bruijn** 474 **graphs**

475 We compare the size of the colored compacted de Bruijn graphs [Iqbal et al., 2012] with that of RLZ-
476 Graphs on human genomic sequences. While there have been many graph construction algorithms
477 for building colored de Bruijn graphs, the graph structure of ccdBG remains the same in these
478 algorithms despite the different approaches to store the reconstruction paths as identifiers in each
479 node. The comparisons made in this section only concern the graph structure, which includes the
480 nodes, edges and the node labels.

481 **8 Experimental results**

482 We use Bifrost [Holley and Melsted, 2020] to construct the ccdBG. The genome graphs constructed
483 include nodes, labels of nodes and edges, are stored in graphical fragment assembly (GFA) for-
484 mat [Li, 2016]. In GFA file, the nodes of a graph are stored as a list of pairs of node identifiers and
485 labels, and edges are stored as a list of pairs of node identifiers. Same as the RLZ-Graph, the graph
486 constructed by Bifrost is bi-directed and does not contain parallel edges. The RLZ-Graph produced
487 in this section does not use the ILP solution to assign sources due to the time and memory concern.
488 Instead, we adopt the leftmost heuristic, where the leftmost source is assigned to each pointer. A
489 source $s_i = (pos_i, len_i)$ is to the left of source $s_j = (pos_j, len_j)$ if $pos_i < pos_j$.

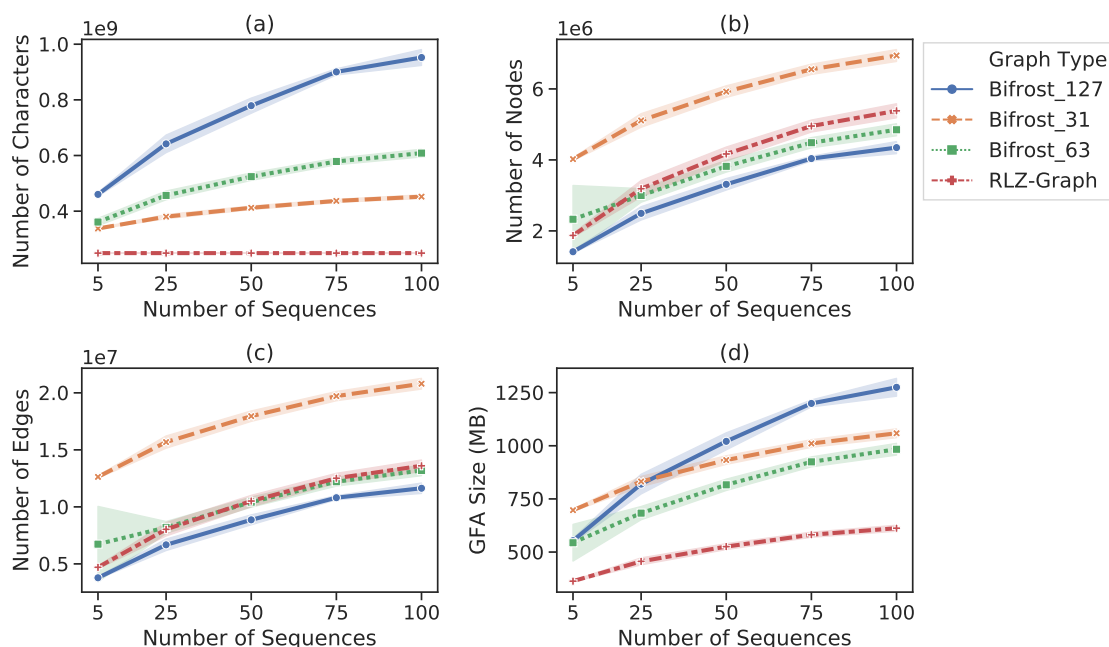


Fig. 5. Comparison between RLZ-Graph and ccDBG constructed by Bifrost with $k = 31, 63$ and 127 on human chromosome 1 sequences. (a) Total number of characters in the node labels. (b) Number of nodes. (c) Number of edges. (d) Size of the GFA file that stores the graph structure and node labels.

490 We build the graphs on all human chromosomes and show the results on chromosome 1 here (see
 491 Supplementary Figure S1-S3 for the rest of the chromosomes). The genomes we use are from the
 492 1000 Genome Project phase 3 [1000 Genomes Project Consortium, 2015]. For each chromosome,
 493 we randomly choose 5, 25, 50, 75 and 100 samples and generate their genomic sequences using the
 494 consensus command from bcftools [Li, 2011]. We construct both graphs using the sample sequences
 495 and the reference hg37. Hg37 is also used as the reference string in RLZ factorization. We vary the
 496 k -mer sizes used for Bifrost and report the sizes of graphs with $k = 31, 63$ and 127 . The default
 497 choice of k of Bifrost is 31. We repeat each experiment 5 times.

498 Shown in Figure 5, we compare the graph size in different aspects. From 5 sequences up to 100
 499 sequences, the graph produced by RLZ-Graph is smaller than the graph produced by Bifrost with
 500 different choices of k under all measures in the figure. At 100 sequences, the GFA file that stores
 501 the RLZ-Graph is 37% smaller than the GFA file storing the colored de Bruijn graph produced by
 502 Bifrost with $k = 63$ and is 42.2% smaller when $k = 31$ (Figure 5(d)). The number of total characters
 503 in the concatenated node labels are constant in the RLZ-Graph regardless of the increase of the
 504 number of sequences because nodes are produced by cutting a reference string.

Table 1. Average wall-clock running time of RLZ-Graph and Bifrost with different k values on chromosome 1 sequences.

Number of sequences	5	25	50	75	100
RLZ-Graph time (s)	1031	2707	4758	6872	9136
Bifrost k=31 time (s)	396	656	986	1542	1852
Bifrost k=63 time (s)	280	510	793	1126	1332
Bifrost k=127 time (s)	412	733	1098	1443	1744

505 The average running time of RLZ-Graph and Bifrost with $k = 31, 63$ and 127 on chromosome 1
506 is reported in Table 1. It takes RLZ-Graph around 2.5 hours to build a graph with 100 chromo-
507 some 1 sequences. The running time includes the time to do RLZ factorization. In all experiments,
508 Bifrost is run in parallel in 20 threads while RLZ-Graph is run in a single thread. The RLZ-Graph
509 implementation is not optimized and not parallelized compared to implementation of Bifrost. Still,
510 the running time is on the similar scale compared to Bifrost.

511 When $k = 15$, the size of the GFA file that stores the ccdBG is 15 gigabytes for 5 chromosome 1
512 sequences and the running time is around 8 hours. Both the size of the graph and the running time
513 is impractical compared to other k values. When $k = 3$, the size of the GFA file is 4.2 kilobytes for
514 5 chromosome 1 sequences with 32 nodes and 127 edges and the running time is around 2.5 hours.
515 Although the graph is small, it is similar to the K_4 solution to the genome graph size optimization
516 problem, where the length of the reconstruction path is approximately the same as the original
517 string. With small k -mers, the ccdBG becomes impractical for human chromosomes. Therefore, we
518 do not include the results of graphs constructed with smaller k values in Figure 5.

519 8.1 Performance of various source assignment heuristics

520 Aside from the ILP solution to the source assignment problem, sources are chosen by other heuristics
521 in literature regarding RLZ factorization [Kuruppu et al., 2011]. Specifically, the leftmost source on
522 the reference string is chosen (Left), or the lexicographically smallest source is chosen (Lex). The
523 lexicographical order of sources of the same source set is defined such that $s_i = (pos_i, len_i) < s_j =$
524 (pos_j, len_j) if $R[pos_i : |R| - 1] < R[pos_j : |R| - 1]$ given a reference string R . In our implementation,
525 a phrase is assigned to its lexicographically smallest source by default. In this section, we compare

526 the performance of different source assignment heuristics in terms of the number of RLZ-Graph
527 nodes in Figure 6(c).

528 We obtain 300 genomic sequences of *E. coli* O157 strain from Genbank [Clark et al., 2016],
529 from which we randomly permute the genomic sequences and construct the RLZ-Graph on varying
530 number of sequences. The first sequence in the randomly permuted 300 sequences is used as the
531 reference string. We repeat each experiment 5 times.

532 In Figure 6(a), we show the rate at which the number of phrases produced by the RLZ factor-
533 ization increases as the number of sequences increases. In Figure 6(b), we show the number of nodes
534 produced due to different source assignment strategies. The ILP solution has the best performance
535 and results in the fewest nodes. The percentage of reduced nodes is around 8% for 300 *E. coli*
536 sequences. As the number of sequences increases, the ILP solution is able to eliminate more nodes
537 compared to the heuristic that always chooses the leftmost source. The percentage of reduced nodes
538 is calculated as $1 - (|V|_{ILP}/|V|_{Left})$ and $1 - (|V|_{Left}/|V|_{Lex})$, respectively.

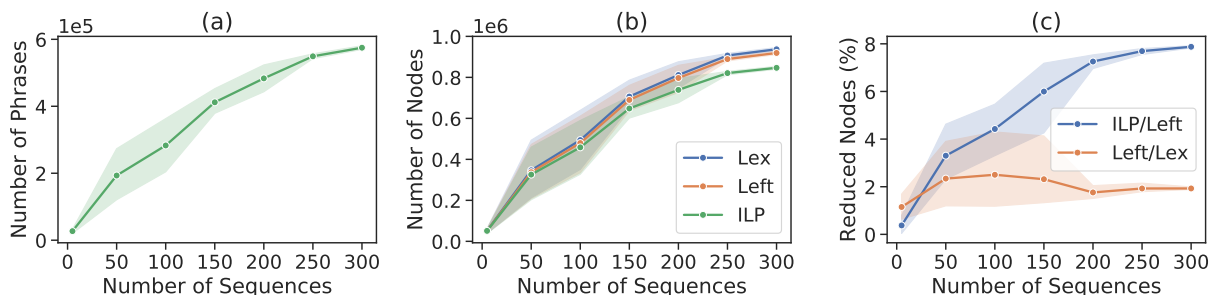


Fig. 6. Performance of heuristics solving the source assignment problem. (a) The number of phrases. (b) The number of nodes. (c) Percentage of nodes reduced using the leftmost heuristic and the ILP solution during the source assignment step. The shaded area in the plots represents the standard deviation across 5 experiments and each data point in the figure represents the mean across 5 experiments. Lex: lexicographical heuristic. Left: leftmost heuristic. ILP: ILP solution.

539 9 Discussion

540 We define the restricted genome graph and formalize the restricted genome graph size optimization
541 problem. The optimization problem balances both the size of the graph structure and the length of
542 the reconstruction paths of sequences stored in the graph, which is similar to the string compression
543 problem. Inspired by the similarity, we present a pair of algorithms that bridge genome graph

544 construction and the external pointer macro model. We prove an upper bound on the size of the
545 genome graph that is constructed based on an optimal compressed string from the EPM model. One
546 key advantage of our graph construction algorithm is that the total number of characters stored in
547 the graph remains the constant regardless of the number of sequences stored in the graph, which
548 helps reduce the space taken by a genome graph. Further, since the number of nodes and edges are
549 derived from an already compressed representation of strings, the number of nodes and the number
550 of edges remain small.

551 We show that equivalent choices made by data compression algorithms may affect the size of the
552 genome graph differently. To address this challenge, we introduce the source assignment problem,
553 and present an ILP solution to it. We show that solving the source assignment problem prior to
554 graph construction reduces the number of nodes by around 8%. Although it is a relatively small
555 percentage, when dealing with very large genome graphs, it translates into substantial space saving.
556 The application of solutions to the source assignment problem is not limited to the relative Lempel-
557 Ziv algorithm, but can be applied to any EPM-compressed form to reduce the number of nodes
558 and edges. The NP-completeness of the source assignment problem is still open.

559 As a proof-of-concept that compressed-based genome graph construction algorithms can produce
560 small genome graphs, we implement RLZ-Graph based on the relative Lempel-Ziv algorithm [Ku-
561 rupp et al., 2010]. We show that using RLZ-Graph, we are able to reduce the size of the graph
562 significantly on disk compared to the colored compacted de Bruijn graph. The choice of k -mer sizes
563 is important in de Bruijn graph construction as it significantly affects the size of the graph. RLZ-
564 Graph removes this dependence on the choice of k and produces practical graphs with a smaller
565 size, which is scalable to the entire human genome. Although the implementation of RLZ-Graph
566 is not optimized, its running time is comparable to the parallelized and optimized ccdBG con-
567 struction method, Bifrost [Holley and Melsted, 2020]. A future direction would be to improve the
568 implementation of RLZ-Graph by parallelizing the RLZ factorization step.

569 This work is an initial investigation into the connection between genome graph construction and
570 string compression. We show that using compression algorithms, we can build small genome graphs
571 efficiently, which opens up the possibilities in future research in adapting other data compression
572 schemes to genome graph construction.

573 **Funding**

574 This work has been supported in part by the Gordon and Betty Moore Foundation's Data-Driven
575 Discovery Initiative through Grant GBMF4554 to C.K., by the US National Institutes of Health
576 (R01GM122935), and the US National Science Foundation (DBI-1937540). Y.Q. was supported by
577 the Carnegie Mellon University School of Computer Science Cancer Research Fellowship for 2021.

578 **Financial Disclosure**

579 C.K. is a co-founder of Ocean Genomics, Inc.

References

- 580
- 581 S. Ballouz, A. Dobin, and J. A. Gillis. Is it time to change the reference genome? *Genome Biology*,
582 20(1):159, 2019.
- 583 Nae-Chyun Chen, Brad Solomon, Taher Mun, Sheila Iyer, and Ben Langmead. Reducing reference
584 bias using multiple population reference genomes. *BioRxiv*, 2020.
- 585 Adam M Novak, Glenn Hickey, Erik Garrison, Sean Blum, Abram Connelly, Alexander Dilthey,
586 Jordan Eizenga, MA Saleh Elmohamed, Sally Guthrie, André Kahles, et al. Genome graphs.
587 *BioRxiv*, page 101378, 2017.
- 588 Benedict Paten, Adam M Novak, Jordan M Eizenga, and Erik Garrison. Genome graphs and the
589 evolution of genome inference. *Genome Research*, 27(5):665–676, 2017.
- 590 Computational Pan-Genomics Consortium. Computational pan-genomics: status, promises and
591 challenges. *Briefings in Bioinformatics*, 19(1):118–135, 2018.
- 592 Rachel M Sherman and Steven L Salzberg. Pan-genomics in the human genome era. *Nature Reviews*
593 *Genetics*, 21(4):243–254, 2020.
- 594 Rachel M Sherman, Juliet Forman, Valentin Antonescu, Daniela Puiu, Michelle Daya, Nicholas
595 Rafaels, Meher Preethi Boorgula, Sameer Chavan, Candelaria Vergara, Victor E Ortega, et al.
596 Assembly of a pan-genome from deep sequencing of 910 humans of african descent. *Nature*
597 *Genetics*, 51(1):30–35, 2019.
- 598 Chirag Jain, Haowen Zhang, Yu Gao, and Srinivas Aluru. On the complexity of sequence to graph
599 alignment. In *International Conference on Research in Computational Molecular Biology*, pages
600 85–100. Springer, 2019.
- 601 Jouni Sirén, Niko Välimäki, and Veli Mäkinen. Indexing graphs for path queries with applications
602 in genome research. *IEEE/ACM Transactions on Computational Biology and Bioinformatics*, 11
603 (2):375–388, 2014.
- 604 Jouni Sirén, Erik Garrison, Adam M Novak, Benedict Paten, and Richard Durbin. Haplotype-aware
605 graph indexes. *Bioinformatics*, 36(2):400–407, 2020.

- 606 Erik Garrison, Jouni Sirén, Adam M Novak, Glenn Hickey, Jordan M Eizenga, Eric T Dawson,
607 William Jones, Shilpa Garg, Charles Markello, Michael F Lin, Benedict Paten, and Richard
608 Durbin. Variation graph toolkit improves read mapping by representing genetic variation in the
609 reference. *Nature Biotechnology*, 36(9):875–879, 2018.
- 610 Heng Li, Xiaowen Feng, and Chong Chu. The design and construction of reference pangenome
611 graphs with minigraph. *Genome Biology*, 21(1):265–283, 2020.
- 612 Benedict Paten, Mark Diekhans, Dent Earl, John St John, Jian Ma, Bernard Suh, and David
613 Haussler. Cactus graphs for genome comparisons. *Journal of Computational Biology*, 18(3):
614 469–481, 2011.
- 615 Veli Mäkinen, Bastien Cazaux, Massimo Equi, Tuukka Norri, and Alexandru I. Tomescu. Linear
616 time construction of indexable founder block graphs. In *20th International Workshop on Algo-*
617 *ritms in Bioinformatics (WABI 2020)*, volume 172 of *Leibniz International Proceedings in In-*
618 *formatics (LIPIcs)*, pages 7:1–7:18, Dagstuhl, Germany, 2020. Schloss Dagstuhl–Leibniz-Zentrum
619 für Informatik.
- 620 Goran Rakocevic, Vladimir Semenyuk, Wan-Ping Lee, James Spencer, John Browning, Ivan J
621 Johnson, Vladan Arsenijevic, Jelena Nadj, Kaushik Ghose, Maria C Suci, et al. Fast and
622 accurate genomic analyses using genome graphs. *Nature Genetics*, 51(2):354–362, 2019.
- 623 Alexander Dilthey, Charles Cox, Zamin Iqbal, Matthew R Nelson, and Gil McVean. Improved
624 genome inference in the MHC using a population reference graph. *Nature Genetics*, 47(6):682–
625 688, 2015.
- 626 Zamin Iqbal, Mario Caccamo, Isaac Turner, Paul Flicek, and Gil McVean. De novo assembly and
627 genotyping of variants using colored de Bruijn graphs. *Nature Genetics*, 44(2):226–232, 2012.
- 628 Jouni Sirén. Indexing variation graphs. In *2017 Proceedings of the nineteenth workshop on algorithm*
629 *engineering and experiments (ALENEX)*, pages 13–27. SIAM, 2017.

- 630 Fatemeh Almodaresi, Prashant Pandey, and Rob Patro. Rainbowfish: a succinct colored de Bruijn
631 graph representation. In *17th International Workshop on Algorithms in Bioinformatics (WABI*
632 *2017)*. Schloss Dagstuhl-Leibniz-Zentrum fuer Informatik, 2017.
- 633 Fatemeh Almodaresi, Prashant Pandey, Michael Ferdman, Rob Johnson, and Rob Patro. An effi-
634 cient, scalable, and exact representation of high-dimensional color information enabled using de
635 Bruijn graph search. *Journal of Computational Biology*, 27(4):485–499, 2020.
- 636 Guillaume Holley and Páll Melsted. Bifrost: highly parallel construction and indexing of colored
637 and compacted de Bruijn graphs. *Genome Biology*, 21(1):249–269, 2020.
- 638 Martin D Muggli, Bahar Alipanahi, and Christina Boucher. Building large updatable colored de
639 Bruijn graphs via merging. *Bioinformatics*, 35(14):i51–i60, 2019.
- 640 Ilia Minkin, Son Pham, and Paul Medvedev. TwoPaCo: an efficient algorithm to build the com-
641 pacted de Bruijn graph from many complete genomes. *Bioinformatics*, 33(24):4024–4032, 2017.
- 642 James A Storer and Thomas G Szymanski. Data compression via textual substitution. *Journal of*
643 *the ACM (JACM)*, 29(4):928–951, 1982.
- 644 Shanika Kuruppu, Simon J. Puglisi, and Justin Zobel. Relative Lempel-Ziv compression of genomes
645 for large-scale storage and retrieval. In Edgar Chavez and Stefano Lonardi, editors, *String Pro-*
646 *cessing and Information Retrieval*, pages 201–206, Berlin, Heidelberg, 2010. Springer Berlin Hei-
647 delberg.
- 648 Sebastian Deorowicz, Agnieszka Danek, and Marcin Niemiec. GDC2: Compression of large collec-
649 tions of genomes. *Scientific Reports*, 5:11565, 2015.
- 650 Sebastian Deorowicz and Szymon Grabowski. Robust relative compression of genomes with random
651 access. *Bioinformatics*, 27(21):2979–2986, 2011.
- 652 Héctor Ferrada, Travis Gagie, Simon Gog, and Simon J Puglisi. Relative Lempel-Ziv with constant-
653 time random access. In *International Symposium on String Processing and Information Retrieval*,
654 pages 13–17. Springer, 2014.

- 655 1000 Genomes Project Consortium. A global reference for human genetic variation. *Nature*, 526
656 (7571):68–74, 2015.
- 657 Travis Gagie, Simon J Puglisi, and Daniel Valenzuela. Analyzing relative Lempel-Ziv reference
658 construction. In *International Symposium on String Processing and Information Retrieval*, pages
659 160–165. Springer, 2016.
- 660 Rajeev Raman, Venkatesh Raman, and S Srinivasa Rao. Succinct indexable dictionaries with
661 applications to encoding k-ary trees and multisets. In *Proceedings of the thirteenth annual ACM-*
662 *SIAM symposium on Discrete algorithms*, pages 233–242. Society for Industrial and Applied
663 Mathematics, 2002.
- 664 Simon Gog, Timo Beller, Alistair Moffat, and Matthias Petri. From theory to practice: Plug and
665 play with succinct data structures. In *13th International Symposium on Experimental Algorithms*,
666 (*SEA 2014*), pages 326–337, 2014.
- 667 Heng Li. Minimap and miniasm: fast mapping and de novo assembly for noisy long sequences.
668 *Bioinformatics*, 32(14):2103–2110, 2016.
- 669 Heng Li. A statistical framework for SNP calling, mutation discovery, association mapping and
670 population genetical parameter estimation from sequencing data. *Bioinformatics*, 27(21):2987–
671 2993, 2011.
- 672 Shanika Kuruppu, Simon J Puglisi, and Justin Zobel. Optimized relative Lempel-Ziv compression of
673 genomes. In *Proceedings of the Thirty-Fourth Australasian Computer Science Conference-Volume*
674 *113*, pages 91–98. Australian Computer Society, Inc., 2011.
- 675 Karen Clark, Ilene Karsch-Mizrachi, David J Lipman, James Ostell, and Eric W Sayers. GenBank.
676 *Nucleic Acids Research*, 44(D1):D67–D72, 2016.

677 **Supplementary results**

678 **1 Comparison between ccdBGs and RLZ-Graphs on human chromosomes**

679 **2–22**

680 We compare the sizes of genome graphs constructed on human chromosomes 2–22 by RLZ-Graph
681 and Bifrost in Figures [S1-S3](#). The experiment settings are the same as in Section [7.1](#) of the main
682 text. Bifrost is run with $k = 31$, which is the default setting.

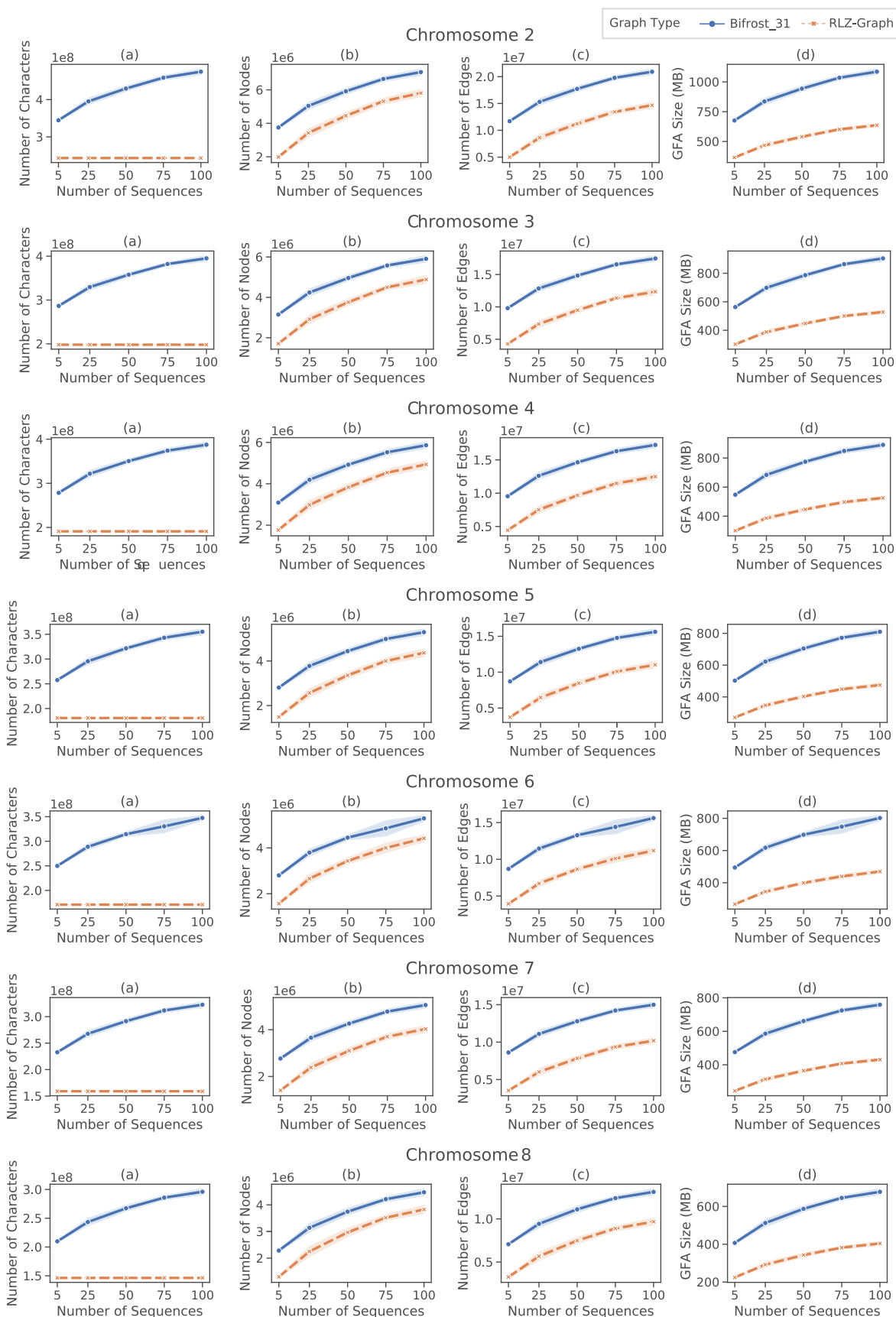


Fig. S1. Comparison between RLZ-Graph and ccdBG constructed by Bifrost with $k = 31$ on human chromosomes 2-8. (a) Total number of characters in the node labels. (b) Number of nodes. (c) Number of edges. (d) Size of GFA file that stores the graph structure and node labels.

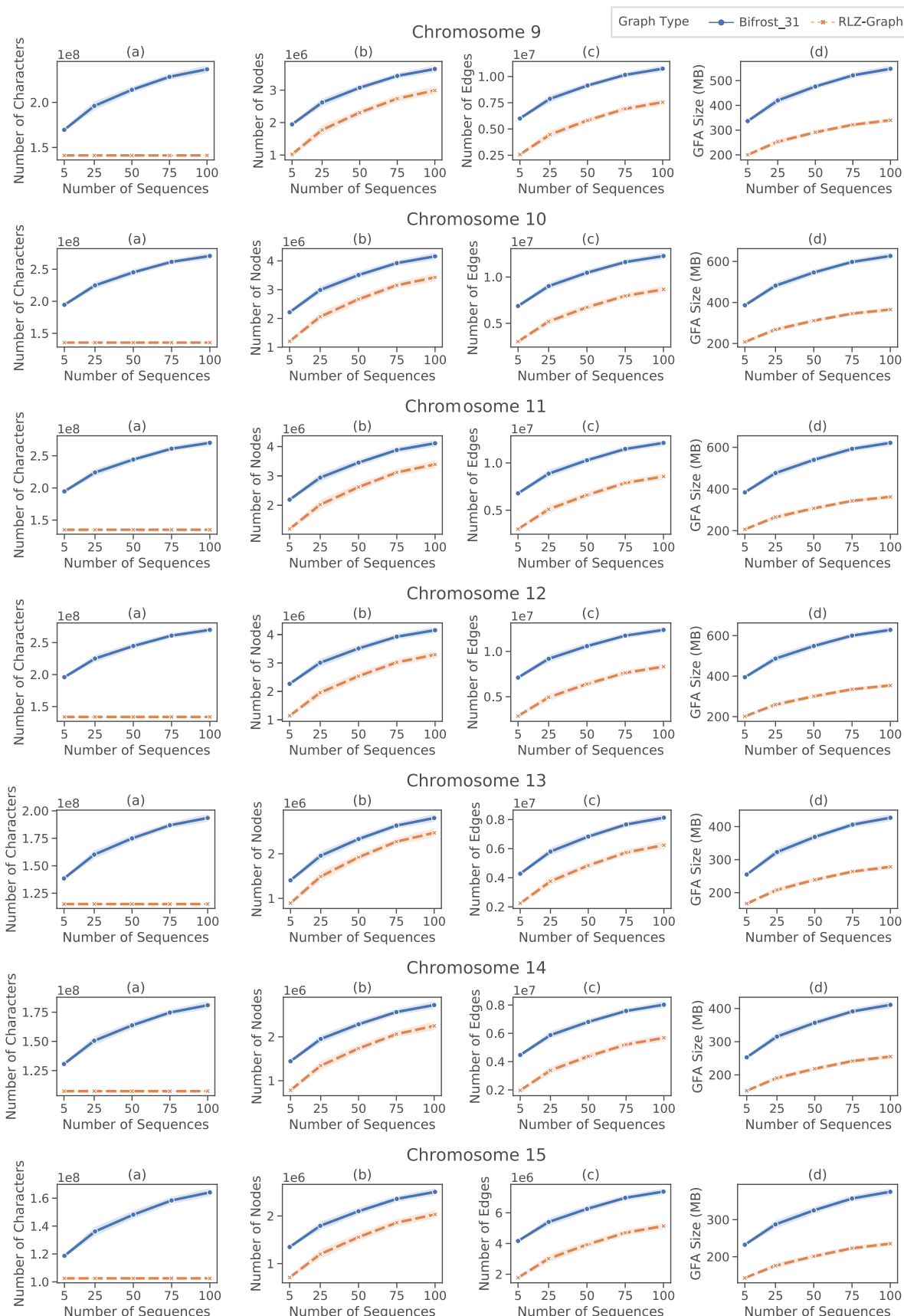


Fig. S2. Comparison between RLZ-Graph and ccdBG constructed by Bifrost with $k = 31$ on human chromosomes 9–15. (a) Total number of characters in the node labels. (b) Number of nodes. (c) Number of edges. (d) Size of GFA file that stores the graph structure and node labels.

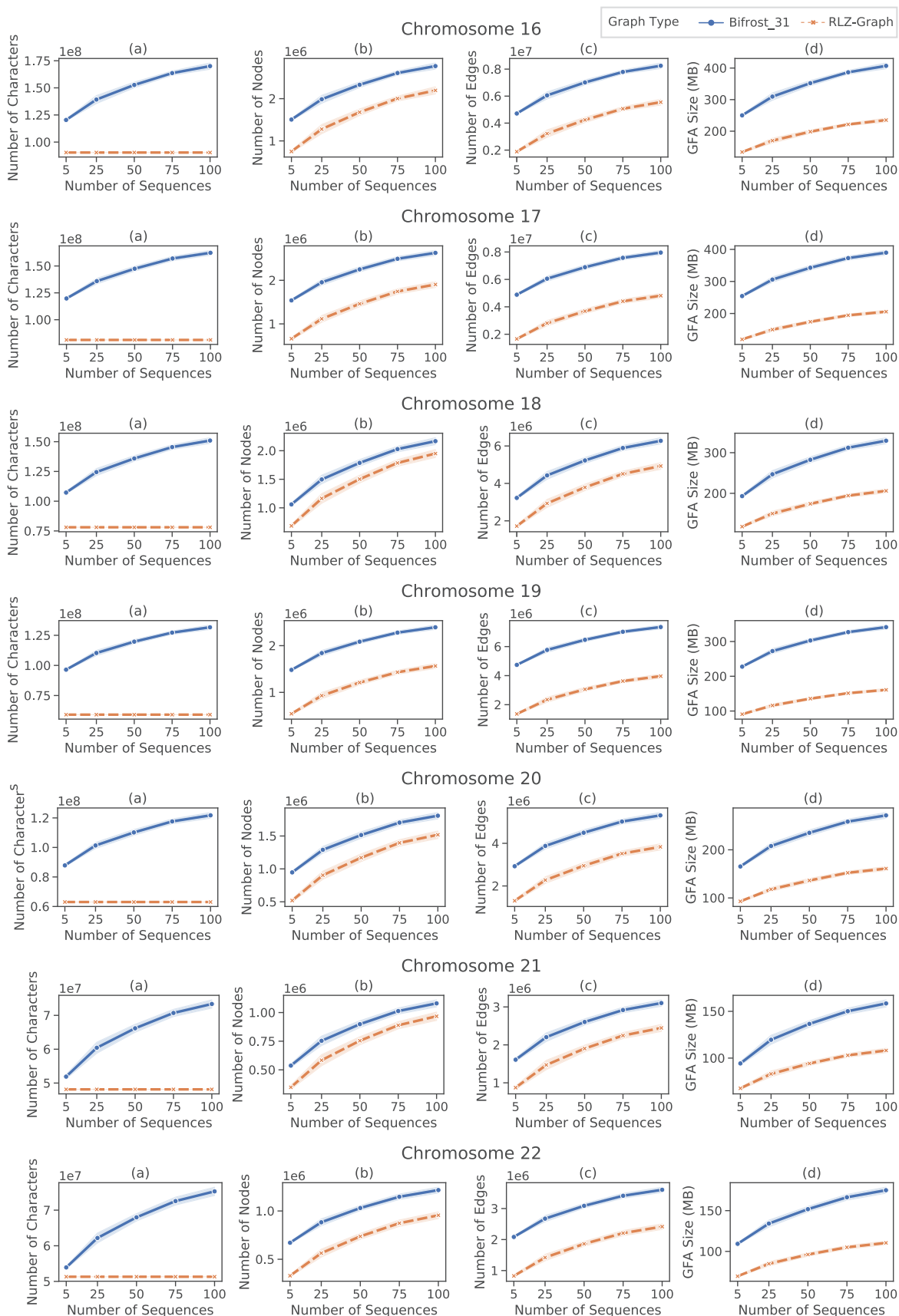


Fig. S3. Comparison between RLZ-Graph and ccdBG constructed by Bifrost with $k = 31$ on human chromosomes 16–22. (a) Total number of characters in the node labels. (b) Number of nodes. (c) Number of edges. (d) Size of GFA file that stores the graph structure and node labels.